Langmuir
Article
pubs.acs.org/Langmuir

Morphological Transitions of Liquid Droplets on Circular Surface Domains

Pedro Blecua,[†] Martin Brinkmann,[‡] Reinhard Lipowsky,[†] and Jan Kierfeld*,[†,§]

[†]*Max Planck Institute of Colloids and Interfaces, Science Park Golm, 14424 Potsdam, Germany,* [‡]*Max Planck Institute for Dynamics and Self-Organization, 37073 Göttingen, Germany, and* [§]*Physics Department, TU Dortmund University, 44221 Dortmund, Germany*

Received June 3, 2009. Revised Manuscript Received July 23, 2009

We study morphological transitions of droplets on a structured substrate containing two circular lyophilic domains for arbitrary domain and substrate wettabilities. We derive the stability criterion that at least one of the droplets must be pinned at the domain boundary with a contact angle smaller than $\pi/2$. This determines seven classes of stable or metastable droplet morphologies of the system. We present a complete classification of stability and metastability of these morphologies as a function of three control parameters as provided by the total droplet volume, substrate wettability, and domain wettability. We find different types of morphological transitions at the stability boundaries: (i) depinning transitions of the contact lines, (ii) symmetry-breaking transitions, where the two droplets acquire different volumes, and (iii) dewetting transitions, where one domain dewets and one of the droplets disappears. We find that depinning transitions of two droplets become discontinuous between two universal values of substrate wettability. Furthermore, below a critical domain wettability, one domain always dewets irrespective of the total volume. We discuss experimental realizations and applications of our results for controlled switching between observed wetting morphologies.

1. Introduction

The study and design of microfluidic systems on the micro- and nanometer scales has important applications in biology, medicine, and chemistry.[1−4] They allow us to handle micro- or nanoliter quantities of reagents while optimizing the reactions and producing the desired products faster and in greater yield and purity.[5]

In open microfluidic systems, a liquid β is deposited on a patterned solid substrate σ, which is in contact with its vapor phase or another immiscible fluid α. For a chemical surface pattern, the equilibrium shape of the liquid droplet is controlled by the shape of the pattern, the wettabilities or contact angles of the surface pattern and substrate, and the total volume V_β of the liquid.[6,7] Depending on these parameters, the liquid droplets can undergo abrupt shape changes or morphological transitions corresponding to bifurcations in shape space. Morphological transitions of single droplets have been theoretically and experimentally studied for a variety of wettability patterns such as arrays of lyophilic circles on a lyophobic substrate,[8] lyophilic and lyophobic stripes,[9−13] and lyophilic rings on a lyophobic background.[14] Abrupt morphological changes are possible if the three-phase contact line is pinned at the domain boundary, which leads to freedom of the contact angle. Often, morphological changes also involve the depinning of the contact line from the domain boundary if the substrate surrounding a surface pattern is sufficiently wettable.[12,14]

Experimental techniques such as microcontact printing[15] or monolayer lithography[16] allow the fabrication of imprinted or structured planar surfaces with tailored chemical patterns of lyophilic and lyophobic surface domains, i.e., exact control of the pattern geometry.[9,10,17] It is much harder, however, to realize specific values of the domain and substrate wettabilities, which are determined by the chemical properties of the surfaces. Therefore, it is necessary to study liquid wetting morphologies for specific substrate patterns for arbitrary, nonspecific values of surface wettability.

In this article, we present such a study of a surface pattern of two circular hydrophilic domains on a hydrophobic (or less hydrophilic) substrate. Droplets on different domains can exchange volume. This system has been studied theoretically in refs 7 and 8 for extreme values of the wettability, i.e., contact angles $\theta_\gamma = 0$ on the domains and $\theta_\delta = \pi$ on the surrounding lyophobic matrix. In this case, the system undergoes a continuous transition between two identical droplets pinned at the domain boundaries and a configuration with two complementary droplets with equal radii of curvature but different volumes; see Figure 1c. This morphological transition occurs at the critical volume where both droplets form two semispherical caps corresponding to a contact angle of $\pi/2$. Because the permutation symmetry between both droplets is broken, we refer to such a transition as a symmetry-breaking transition (SBT) in the following text. For three or more droplets, the corresponding SBT becomes discontinuous.[8] Similar symmetry-breaking transitions for soap bubbles have been studied in ref 18. Experimental realizations of this SBT

*Corresponding author. E-mail: jan.kierfeld@tu-dortmund.de.

(1) Squires, T.; Quake, S. *Rev. Mod. Phys.* **2005**, *77*, 977–1026.
(2) Ramsey, J.; Jacobson, S.; Knapp, M. *Nat. Med.* **1995**, *1*, 1093–1096.
(3) Whitesides, G.; Ostuni, E.; Takayama, S.; Jinag, X.; Ingber, D. *Annu. Rev. Biomed. Eng* **2001**, *3*, 335–373.
(4) Beebe, D.; Mensing, G.; Walker, G. *Annu. Rev. Biomed. Eng* **2002**, *4*, 261–286.
(5) Dubois, P.; Marchand, G.; Fouillet, Y.; Berthier, J.; Douki, T.; Hassine, F.; Gmouth, S.; Vaultier, M. *Anal. Chem.* **2006**, *78*, 4909–4917.
(6) Lipowsky, R.; Lenz, P.; Swain, P. *Colloids Surf., A* **2000**, *161*, 3–22.
(7) Lipowsky, R.; Brinkmann, M.; Dimova, R.; Haluska, C.; Kierfeld, J.; Shillcock, J. *J. Phys: Condens. Matter* **2005**, *17*, S2885–S2902.
(8) Lenz, P.; Lipowsky, R. *Phys. Rev. Lett.* **1998**, *80*, 1920–1923.
(9) Gau, H.; Herminghaus, S.; Lenz, P.; Lipowsky, R. *Science* **1999**, *283*, 46–49.
(10) Kataoka, D.; Troian, S. *Nature* **1999**, *402*, 794–797.
(11) Darhuber, A.; Troian, S.; Miller, S.; Wagner, S. *J. Appl. Phys.* **2000**, *87*, 7768.–7775.
(12) Brinkmann, M.; Lipowsky, R. *J. Appl. Phys.* **2002**, *92*, 4296–4306.
(13) Klingner, A.; Mugele, F. *J. Appl. Phys.* **2004**, *95*, 2918–2920.
(14) Lenz, P.; Fenzl, W.; Lipowsky, R. *Europhys. Lett.* **2001**, *53*, 618–624.
(15) Xia, Y.; Whitesides, G. *Angew. Chem., Int. Ed.* **1998**, *37*, 550–574.
(16) Burmeister, F.; Schäfle, C.; Matthes, T.; Böhmisch, M.; Boneberg, J.; Leiderer, P. *Langmuir* **1997**, *13*, 2983–2987.
(17) Wang, J.; Zheng, Z.; Li, H.; Huck, W.; Sirringhaus, H. *Nat. Mater.* **2004**, *3*, 171–176.
(18) Wente, H. *Pac. J. Math.* **1999**, *189*, 339–375.

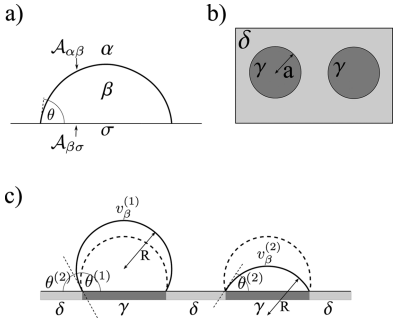

Figure 1. (a) Side view of a spherical droplet on a homogeneous substrate σ. (b) Top view of two circular lyophilic domains γ embedded in a lyophobic substrate δ. (c) Side view of two complementary droplets with equal radii of curvature R but different dimensionless volumes $v_\beta^{(1)} > v_\beta^{(2)}$ on two identical lyophilic circular domains γ embedded in a lyophobic matrix δ and in contact with the same vapor phase α (solid lines). This is the equilibrium configuration in regime 2C, where the total volume has been increased beyond the critical value for the continuous symmetry-breaking transition (SBT). State 2S with two symmetric droplets with the same total volume (dashed lines) is energetically unfavorable.

for droplets pinned at communicating circular orifices, the theoretical description of which is analogous to the case of droplets on two domains with extreme wettabilities, have been reported in refs 19−21 Moreover, these experimental realizations allow for controlled switching between degenerate morphologies with broken symmetry by electroosmosis[19] or pressure pulses.[20,21]

Here, we generalize the results of refs 7 and 8 to *arbitrary* contact angles θ_γ and θ_δ. We derive the stability criterion that at least one of the droplets must be pinned at the domain boundary with a contact angle smaller than $\pi/2$. This allows us to classify all (meta)stable droplet morphologies into seven possible regimes; see Figure 2. These include single-droplet configurations, where one domain is dewetted as in regimes I, II, and III (Figure 2), and two-droplet configurations, where one of the droplets is depinned from the domain boundary (regimes 4 and 5 in Figure 2). Therefore, we also find additional classes of morphological transitions apart from the SBT: depinning transitions of the contact lines and dewetting transitions, at which one of the droplets disappears. We predict several remarkable features for these transitions, which should be accessible to experimental testing: (i) Depinning transitions for two droplets can be either continuous or discontinuous. They become discontinuous between two universal values of substrate wettability. (ii) For sufficiently low contact angles θ_δ, symmetry breaking and depinning take place simultaneously in a single transition. (iii) Below a critical domain wettability, i.e., for sufficiently large contact angles θ_γ, one of the domains dewets independently of the total droplet volume. The corresponding dewetting transition is discontinuous.

The article is organized as follows. In section 2, we present the geometric interface model for fluids wetting a structured substrate. In section 3, we present the stability criterion based on the volume dependence of the Laplace pressure and classify all possible stable or metastable morphologies of the system. In section 4, we present morphology and stability diagrams and discuss all types of morphological transitions: pinning and depinning transitions of

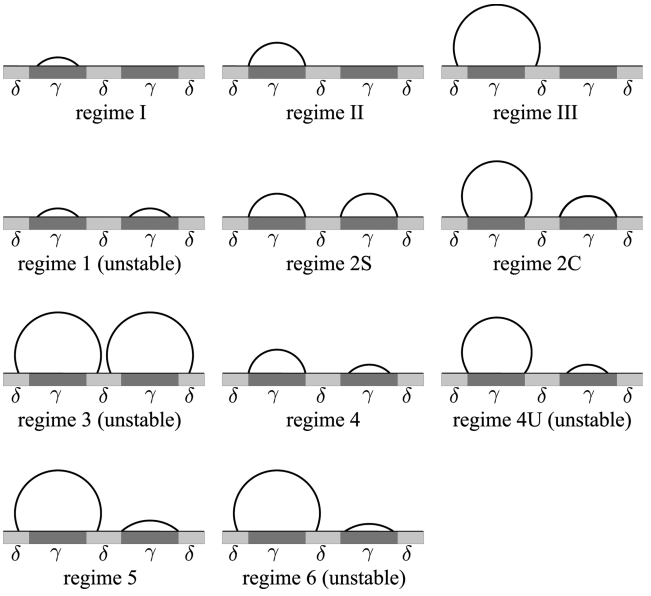

Figure 2. Eleven droplet morphologies that are permitted by the contact angle equation (eq 3) and the condition of equal Laplace pressures or mean curvatures for liquid droplets (β) on two identical lyophilic circular domains γ, embedded in a more lyophobic matrix δ. Droplets can exchange volume, for example, via the surrounding vapor phase. There are three single-droplet regimes:[6,7] regime I with $\theta = \theta_\gamma$, regime II with $\theta_\gamma \le \theta \le \theta_\delta$, and regime III with $\theta = \theta_\delta$. There are four analogous regimes for two droplets: regime 1 with both droplets in regime I, regimes 2S and 2C with both droplets in regime II, and regime 3 with both droplets in regime III. In regime 2S (where S stands for symmetric), we have two identical caps; in regime 2C (where C stands for complementary), we have two complementary spherical caps, i.e., $\theta^{(2)} = \pi - \theta^{(1)}$. Finally, we have four more possible morphologies, which we call regime 4 with one droplet in regime I and one droplet in regime II (two cases in which the contact angle of the pinned droplet is smaller or larger than $\pi/2$), regime 5 with one droplet in regime II and one droplet in regime III, and regime 6 with one droplet in regime I and one droplet in regime III. Regimes 1, 3, and 6 give unstable droplet configurations, and regime 4U is unstable because the contact angle of the pinned droplet exceeds $\pi/2$.

the contact lines, symmetry-breaking transitions, and dewetting transitions. We also present all instability lines associated with discontinuous transitions and additional transitions between metastable states. Finally, we discuss experimental implications of our theoretical work in section 5. In the main text, we focus on the discussion of our results; a complete derivation of these results is given in the Supporting Information.

2. Model

2.1. Free Energy. We consider a chemically structured substrate consisting of two identical circular lyophilic domains γ of radius a, embedded in a more lyophobic substrate δ. Droplets of a liquid β are placed on these domains in contact with the vapor phase or another immiscible fluid α; see Figure 1a. The two droplets can exchange volume; see Figure 1b,c. Because volume exchange via the surrounding vapor phase is slow, we discuss other experimental realizations in the last section of the article that could allow for fast volume exchange. Our analysis is based on the minimization of the interfacial free energies associated with the $\alpha\beta$ interface and the $\alpha\sigma$ contact surface with the substrate.

2.1.1. Single Droplet. First, we consider the free energy of a single droplet bounded by an $\alpha\beta$ interface with area $A_{\alpha\beta}$ and a contact surface $\mathcal{A}_{\beta\sigma}$ with area $A_{\beta\sigma}$, which meet in the three-phase

(19) Vogel, M.; Ehrhard, P.; Steen, P. *Proc. Natl. Acad. Sci. U.S.A.* **2005**, *102*, 11974–11979.
(20) Hirsa, A.; López, C.; Laytin, M.; Vogel, M.; Steen, P. *Appl. Phys. Lett.* **2005**, *86*, 014106.
(21) Theisen, E.; Vogel, M.; López, C.; Hirsa, A.; Steen, P. *J. Fluid Mech.* **2007**, *580*, 495–505.

contact line; see Figure 1a. On a chemically heterogeneous substrate, both surface tensions $\Sigma_{\alpha\sigma}(\mathbf{x})$ and $\Sigma_{\beta\sigma}(\mathbf{x})$ are functions of the position $\mathbf{x}$ on the substrate. The free energy of a droplet with fixed volume V_β on a chemically heterogeneous substrate assumes the form[6,12]

$$\mathcal{F} = \Sigma_{\alpha\beta} A_{\alpha\beta} + \int_{\mathcal{M}_{\beta\sigma}} \mathrm{d}A[\Sigma_{\beta\sigma}(\mathbf{x}) - \Sigma_{\alpha\sigma}(\mathbf{x})] \tag{1}$$

Apart from the linear size $\propto V_\beta^{1/3}$ of the droplet, the free energy of a droplet contains a number of different length scales associated with gravity, molecular distances, interfacial widths, critical correlations of the wetting transition, and line tension.[6] We focus on droplet sizes in the millimeter range, which are large enough to ignore effects from molecular distances, the interface width, and the correlation length in the liquid phase and are small enough to ignore effects from gravity. Gravity effects can be ignored for droplets that are small compared to the so-called capillary length. For water at room temperature, the capillary length is 3.8 mm. Furthermore, we ignore effects from the line tension associated with the three-phase contact line, which have been discussed in detail for a single lyophilic circular domain in ref 22 and can become relevant for nanometer-sized droplets.

For locally stable equilibrium morphologies, the first variation of the free energy (eq 1) vanishes with respect to small displacements of the $\alpha\beta$ interface and associated displacements of the three-phase contact line. The first variation is taken under the constraint of fixed volume V_β. This constraint is implemented using a Lagrange multiplier ΔP, which assumes the meaning of a Laplace pressure $P_{\mathrm{La}} \equiv \Delta P = P_\beta - P_\alpha$, where P_α and P_β are the α and β phase bulk pressures, respectively. Local equilibrium with respect to displacements of the $\alpha\beta$ interface leads to the Laplace equation

$$2M\Sigma_{\alpha\beta} = P_{\mathrm{La}} = P_\beta - P_\alpha \tag{2}$$

where M is the mean curvature of the $\alpha\beta$ interface. According to the Laplace equation (eq 2), the droplet attains a shape of constant mean curvature, which is a spherical cap on a homogeneous substrate. Local equilibrium with respect to displacements of the three-phase contact line leads to the contact line equation[8]

$$\cos\theta = w(\mathbf{x}) \tag{3}$$

where θ is the local contact angle and where we introduced the position-dependent wettability

$$w(\mathbf{x}) \equiv \frac{\Sigma_{\alpha\sigma}(\mathbf{x}) - \Sigma_{\beta\sigma}(\mathbf{x})}{\Sigma_{\alpha\beta}} \tag{4}$$

Complete wetting is reached when $w = 1$ or $\theta = 0$, and partial wetting occurs when $-1 < w < 1$ or $0 < \theta < \pi$. Both Laplace and contact line equations describe locally stable configurations of the droplet. In the present study, the wettability w can be regarded as short-hand notation for $\cos\theta$. If we included line tension effects, then we would have to distinguish between these two quantities because w is then only one contribution to $\cos\theta$; see refs 6 and 22.

For a patterned surface with a single circular lyophilic domain, both the Laplace equation (eq 2) and the circular surface pattern are compatible with droplet shapes consisting of spherical caps. Using a general stability criterion that has been derived in refs 23 and 24, it has been shown for droplets on homogeneous substrates that spherical caps represent stable minima of the free energy (eq 1) with respect to *arbitrary* shape variations.[25] The stability criterion of refs 23 and 24 suggests that this result also holds in the presence of a circular surface pattern if the surface becomes less lyophilic with increasing distance from the center, as is the case for a single circular lyophilic domain. For such spherical caps, there are the three regimes I, II, and III of wetting behavior; see Figure 2. The contact angle equation (eq 3) is fulfilled in regime I, where the droplet is entirely within domain γ and the contact angle is given by $\cos\theta_\gamma = w_\gamma$, and in regime III, where the droplet wets the surrounding δ substrate and the contact angle is given by $\cos\theta_\gamma = w_\delta$. Because we consider piecewise constant wettabilities, i.e., w_γ inside the domain and w_δ outside, the three-phase contact line of the droplet is pinned at the boundary of the domain in regime II. Because of this pinning of the contact line, there is freedom of the contact angle, which can attain arbitrary values in the range of $\theta_\gamma \le \theta \le \theta_\delta$.[8]

We can express the free energy for a single droplet as given in eq 1 in each of the three regimes in terms of the droplet volume. We first define a dimensionless free energy and a dimensionless volume via

$$f \equiv F/2\pi\Sigma_{\alpha\beta}a^2 \quad \text{and} \tag{5}$$

$$v_\beta \equiv V_\beta/(2\pi/3)a^3 \tag{6}$$

We measure free energies in units of the surface energy of the $\alpha\beta$ interface of a half sphere and droplet volumes in units of the volume of such a half sphere.

Using eq 1 for a fixed volume together with the relations $A_{\alpha\beta} = 2\pi R^2(1-\cos\theta)$, $A_{\beta\sigma} = \pi R^2 \sin^2\theta$, and $V_\beta = {}^{\pi}/_{3}\, R^3(1-\cos\theta)^2 \times (2+\cos\theta)$ as appropriate for spherical caps with a radius of curvature R and a contact angle θ and making use of the contact angle equation (eq 3), we end up with

$$f_{\mathrm{I}}(v_\beta) = \frac{1}{2}(2v_\beta)^{2/3}(2 - 3w_\gamma + {w_\gamma}^3)^{1/3} \tag{7}$$

$$f_{\mathrm{III}}(v_\beta) = \frac{1}{2}(2v_\beta)^{2/3}(2 - 3w_\delta + {w_\delta}^3)^{1/3} + \frac{1}{2}(w_\delta - w_\gamma) \tag{8}$$

for regimes I and III, respectively. In regime II, we cannot use the contact angle equation (eq 3) but have the additional constraint $a = R\sin\theta$, which gives the pair of equations

$$f_{\mathrm{II}}(\cos\theta) = \frac{1}{1+\cos\theta} - \frac{1}{2}w_\gamma \tag{9}$$

$$v_\beta = \frac{1}{2}\,\frac{2 - 3\cos\theta + \cos^3\theta}{\sin^3\theta} \tag{10}$$

which can be solved explicitly for the volume dependence $f_{\mathrm{II}}(v_\beta)$; see Supporting Information.

(22) Blecua, P.; Lipowsky, R.; Kierfeld, J. *Langmuir* **2006**, *22*, 11041–11059.

(23) Rosso, R.; Virga, E. *Phys. Rev. E* **2003**, *68*, 012601.

(24) Brinkmann, M.; Kierfeld, J.; Lipowsky, R. *J. Phys. A: Math. Gen.* **2004**, *37*, 11547–11573.

(25) Guzzardi, L.; Rosso, R.; Virga, E. *Phys. Rev. E* **2006**, *73*, 021602.

The volumes at which the droplet gets pinned or at which it depins to or from the boundary of the circular domain for increasing droplet volume are given by

$$v_{\beta,\mathrm{pin}} = \frac{1}{2}\,\frac{2-3w_\gamma+{w_\gamma}^3}{(1-{w_\gamma}^2)^{3/2}} \tag{11}$$

$$v_{\beta,\mathrm{dep}} = \frac{1}{2}\,\frac{2-3w_\delta+{w_\delta}^3}{(1-{w_\delta}^2)^{3/2}} \tag{12}$$

respectively. Now, we have explicit expressions for the free energy of a single droplet $f = f(v_\beta)$ through all three wetting regimes: eq 7 applies in regime I for $v_\beta < v_{\beta,\mathrm{pin}}$, eqs 9 and 10 apply in regime II for $v_{\beta,\mathrm{pin}} < v_\beta < v_{\beta,\mathrm{dep}}$, and eq 8 applies in regime III for $v_\beta > v_{\beta,\mathrm{dep}}$.

2.1.2. Two Droplets. For two droplets (1 and 2) on two identical lyophilic circular domains with volumes $v_\beta^{(1)}$ and $v_\beta^{(2)}$ (Figure 1c), which can exchange volume but have a fixed total volume of $v_\beta = v_\beta^{(1)} + v_\beta^{(2)}$, the total free energy is given by

$$f_{2d}(v_\beta, v_\beta^{(1)}) = f(v_\beta^{(1)}) + f(v_\beta - v_\beta^{(1)}) \tag{13}$$

with the free energy $f(v_\beta)$ of a single droplet in regimes I, II, or III as derived in the previous section.

Because each of the spherical caps is stable with respect to any volume preserving shape variation, the total free energy (eq 13) represents the restricted free energy minimum of the droplets for given values of both v_β and $v_\beta^{(1)}$. Under volume exchange, the restriction on volume $v_\beta^{(1)}$ is lifted, and $v_\beta^{(1)}$ will assume a value that minimizes the total free energy (eq 13) for given wettabilities and total volume v_β. Thus, all of the equilibrium configurations can be found by varying the total free energy (eq 13) with respect to $v_\beta^{(1)}$. We can classify the morphological transitions between different stable (or metastable) equilibrium states by following these stationary states as a function of the total volume v_β or the wettabilities w_γ and w_δ. In all possible local equilibrium states containing two droplets, the condition $\partial f_{2d}/\partial v_\beta^{(1)} = 0$ is fulfilled. This implies that both droplets have equal Laplace pressures or equal radii of curvature. We also note that both droplets in eq 13 fulfill the contact angle equation (eq 3) by construction of the free energy $f(v_\beta)$ of a single droplet.

3. Stability Criterion and Possible Morphologies

3.1. Stability Criterion. For two droplets, which can exchange volume, the condition of equal Laplace pressures is complemented by the following necessary stability criterion:

States with two droplets can be stable only if at least one of the droplets is pinned at the corresponding domain boundary and has a contact angle of $\theta < \pi/2$. (14)

This additional stability criterion arises from the volume dependence of the Laplace pressure of the droplets, and a detailed derivation is given in the Supporting Information. The criterion is based on the observation that on monotonically decreasing branches of the Laplace pressure for a single droplet as a function of its volume, volume exchange with a second droplet leads to an instability: If a small volume is removed from the droplet, then the Laplace pressure increases and the volume of the droplet tends to decrease further. Monotonically increasing and, thus, stabilizing branches of the Laplace pressure exist only for a pinned droplet with a contact angle of $\theta < {}^{\pi}/_{2}$.

The criterion (eq 14) can also be generalized to systems involving an *arbitrary* number of N circular domains with $M \leq N$ droplets, which can exchange volume: States containing $M > 1$ droplets can be stable only if at least $M - 1$ of the droplets are pinned and have a contact angle of $\theta < {}^{\pi}/_{2}$. Otherwise, a pair of droplets can be found that become unstable under volume exchange.

3.2. Possible Morphologies. For two droplets sitting on two identical lyophilic circular domains of radius a, we can have a variety of possible morphologies, which fulfill both the contact angle equation (eq 3) and the condition of equal Laplace pressures, i.e., equal radii of curvature, as shown in Figure 2.

Apart from the situation where we have only one droplet and the corresponding three single-droplet regimes I, II, and III, we can have three analogous regimes for two droplets: regime 1 with two identical droplets in regime I, i.e., sitting inside γ domains, regime 3 with two identical droplets in regime III wetting the surrounding lyophobic matrix, and regime 2, where two droplets are in regime II with both of them pinned at the domain boundary. In this latter regime 2, we can have two possible equilibrium morphologies: a symmetric configuration with two identical droplets (regime 2S) or a nonsymmetric configuration with two complementary caps (regime 2C); see Figure 2. Both droplets consist of the β phase and are in coexistence (or close to coexistence) with the same α phase. As stated above, the radii of curvature of the two droplets must then be equal; because both droplets are pinned to the boundary, the droplets have equal contact angles of $\theta^{(1)} = \theta^{(2)}$ in 2S and complementary contact angles of $\theta^{(1)} = \pi - \theta^{(2)}$ in 2C.[6,7]

Finally, three additional morphologies can occur, and define the regimes 4, 5, and 6; see Figure 2. In regime 4, the larger droplet is pinned to the boundary, while the other one lies inside the γ domain with equal radius of curvature. The pinned droplet can have both contact angles larger or smaller than ${}^{\pi}/_{2}$. In regime 5, the smaller droplet remains pinned to the boundary, while the other one wets the surrounding lyophobic matrix. For equal radii of curvature the pinned droplet must have a contact angle smaller than ${}^{\pi}/_{2}$. And in regime 6, the larger droplet wets the surrounding matrix, while the smaller one lies inside the domain with equal radius of curvature.

By applying our additional stability criterion (eq 14), we can identify the possible (meta)stable morphologies. As stated, only the regimes in which at least one droplet is pinned with contact angle $\theta < {}^{\pi}/_{2}$ can be (meta)stable. This criterion implies that droplets in regime 1, 3, and 6 are unstable because there are no pinned droplets. In regime 4, configurations with the contact angle of the pinned larger droplet larger than ${}^{\pi}/_{2}$ are unstable and give rise to regime 4U, whereas configurations with a contact angle of the pinned droplet smaller than ${}^{\pi}/_{2}$ can be metastable. Apart from regimes I, II, and III with a single droplet, we are thus left with four additional possible metastable morphologies: two equal droplets pinned (regime 2S), two complementary droplets pinned (regime 2C), only the larger droplet pinned with $\theta < {}^{\pi}/_{2}$ (regime 4), and only the smaller droplet pinned (regime 5). Hence, up to seven stable or metastable morphologies are possible.

4. Morphology and Stability Diagrams

In this section, we will discuss the possible (meta)stable wetting morphologies and transitions between these morphologies as a function of several experimentally accessible control parameters, the wettabilities w_γ and w_δ, and the total volume v_β. We want to consider arbitrary wettabilities and will assume only that the

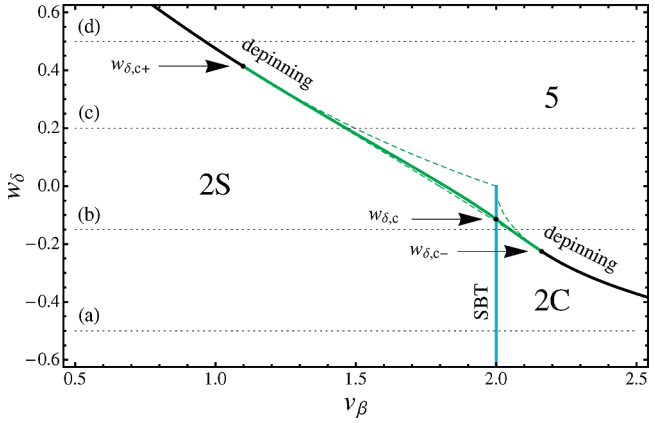

Figure 3. Morphology and stability diagram in the (ν_β, w_δ) plane for $w_\gamma = 1$. Because of $w_\gamma = 1$, the morphology diagram exhibits only the three two-droplet morphologies 2S, 2C, and 5 as described in Figure 2. There are symmetry-breaking and depinning transitions between these two-droplet regimes. The depinning transition lines between regimes 2S and 5 and between regimes 2C and 5 are shown as black solid lines where the depinning transition is continuous and as solid green lines where it is discontinuous. The lines meet at tricritical points $w_{\delta,c+} = -1 + 2^{1/2}$ and $w_{\delta,c-} \simeq -0.225$ (arrows). The dashed green lines show the corresponding instability lines of the discontinuous transition. The solid turquoise line $\nu_{\beta,SBT} = 2$ is the SBT line, which intersects the discontinuous depinning transition lines at the critical endpoint $w_{\delta,c} = {}^1/_{10}(6 - 51^{1/2}) \simeq -0.114$ (arrow). In Figures 4 and 5, we show morphology and stability diagrams in the (ν_β, w_γ) plane for the four representative values of w_δ, which are indicated by horizontal dotted lines: (a) $w_\delta = -0.5 < w_{\delta,c-}$, (b) $w_\delta = -0.15$ with $w_{\delta,c-} < w_\delta < w_{\delta,c}$, (c) $w_\delta = -0.2$ with $w_{\delta,c} < w_\delta < w_{\delta,c+}$, and (d) $w_\delta = 0.5 > w_{\delta,c+}$.

γ domains are lyophilic and that they are more lyophilic than the δ substrate,

$$w_\gamma = \cos\theta_\gamma > 0 \quad \text{and} \quad w_\gamma = \cos\theta_\gamma > \cos\theta_\delta = w_\delta \qquad (15)$$

in the following text. Our results are summarized in a series of morphology and stability diagrams.

For each of the possible (meta)stable regimes, the free energy is derived as a function of the wettabilities w_γ and w_δ and the volume ν_β; see the Supporting Information. A morphological transition between two morphologies takes place when the corresponding branches of the free energy as a function of the total volume ν_β intersect. This determines the location of the morphological transition lines in the parameter space spanned by w_γ, w_δ, and ν_β. A morphology looses its stability if the corresponding free-energy branch ends because the corresponding local minimum in the restricted free energy $f(\nu_\beta) = \min_{\nu_\beta^{(1)}}[f_{2d}(\nu_\beta, \nu_\beta^{(1)})]$ (eq 13) vanishes in a bifurcation. This determines the instability (or spinodal) lines for each regime. In the Supporting Information, we present the details of the derivation of all transition and stability lines. Here we will give the main results, which are relevant to experimental applications. The morphological transition lines between the seven regimes are displayed in morphology diagrams, and the corresponding instability lines are displayed in stability diagrams.

In the morphology diagrams, the transition lines between stable regimes are shown as a function of the wettability w_γ (Figure 4) or w_δ (Figure 3) and the total volume ν_β. In a typical experiment, the wettabilities are fixed by the surface chemistry of the substrate. For the given wettabilities, it is then possible to follow a horizontal line in the diagram by changing the total volume ν_β. Thermal fluctuations are usually weak such that there are pronounced hysteresis effects at discontinuous morphological transitions. The system remains in a metastable configuration until it becomes unstable even if the stable state with the global energy minimum has already changed. Therefore, the stability diagrams that display the instability (or spinodal) lines (Figure 5) are as important as the corresponding morphology diagrams. Furthermore, there can be transitions between two *metastable* morphologies if the corresponding metastable free-energy branches intersect. Such transitions are also indicated in the stability diagrams.

We find three classes of phase transitions: (i) depinning transitions of the contact lines, (ii) symmetry-breaking transitions, where the two droplets acquire different volumes and (iii) dewetting transitions, where one domain dewets and one of the droplets vanishes. We will show that depinning transitions between two-droplet morphologies can be continuous *or* discontinuous depending on the substrate wettability. In contrast, symmetry-breaking transitions are always continuous, and dewetting transitions are always discontinuous.

For an extremely lyophobic substrate with wettability $w_\delta = -1$, depinning transitions where the contact lines moves onto the δ substrate are suppressed. For an extremely lyophilic domain with wettability $w_\gamma = 1$, dewetting of any domain and, thus, single-droplet morphologies are suppressed. If both $w_\delta = -1$ and $w_\gamma = 1$, then we only find a single symmetry-breaking transition.[8] To investigate the interplay of depinning, symmetry-breaking, and dewetting transitions of two droplets, it is useful to consider first depinning and symmetry-breaking transitions, which are classified in a morphology diagram (Figure 3) in the (ν_β, w_δ) plane for extreme domain wettability $w_\gamma = 1$ such that dewetting is suppressed and we always have two droplets. In the next step, we then focus on additional dewetting transitions between double- and single-droplet morphologies, which leads to several morphology and stability diagrams (Figures 4 and 5) in the (ν_β, w_γ) plane for representative values of w_δ.

4.1. Depinning Transitions between Single-Droplet Morphologies. A single droplet can be in regime I, II, or III wetting only one of the domains. In that case, the transitions from one morphology to the other are pinning or depinning transitions where the contact line pins to or depins from the domain boundary. These transitions are continuous (as long as we ignore possible line tension effects, see ref 22). The depinning transition from morphology I to morphology II takes place at volume $\nu_{\beta,pin}$ (eq 11), and the depinning transition from morphology II to morphology III takes place at volume $\nu_{\beta,dep}$ (eq 12). They are represented by the solid blue lines in the morphology diagrams in Figure 4. The depinning transition line between regimes I and II depends only on the domain wettability w_γ. Likewise, the depinning transition line between regimes II and III depends only on the substrate wettability w_δ and therefore gives vertical lines in the morphology diagrams in Figure 4 in the (ν_β, w_γ) plane.

4.2. Transitions between Two-Droplet Morphologies. Transitions between two different two-droplet morphologies are either symmetry-breaking transitions (SBTs), where the permutation symmetry of the two droplets is lost, or depinning transitions, where a pinned droplet spreads onto the δ substrate or retracts onto the γ domain or combinations of both types.

In principle, transitions between different two-droplet morphologies can be analyzed by studying bifurcations of the corresponding free-energy branches $f_{2S}(\nu_\beta)$, $f_{2C}(\nu_\beta)$, $f_4(\nu_\beta)$, and $f_5(\nu_\beta)$. For the two-droplet regimes, this bifurcation analysis of the free energies is difficult because we have only parametric representations of $f_4(\nu_\beta)$ and $f_5(\nu_\beta)$ in terms of the parameter $\cos\theta^{(1)}$, where $\theta^{(1)}$ is the contact angle of the pinned droplet.

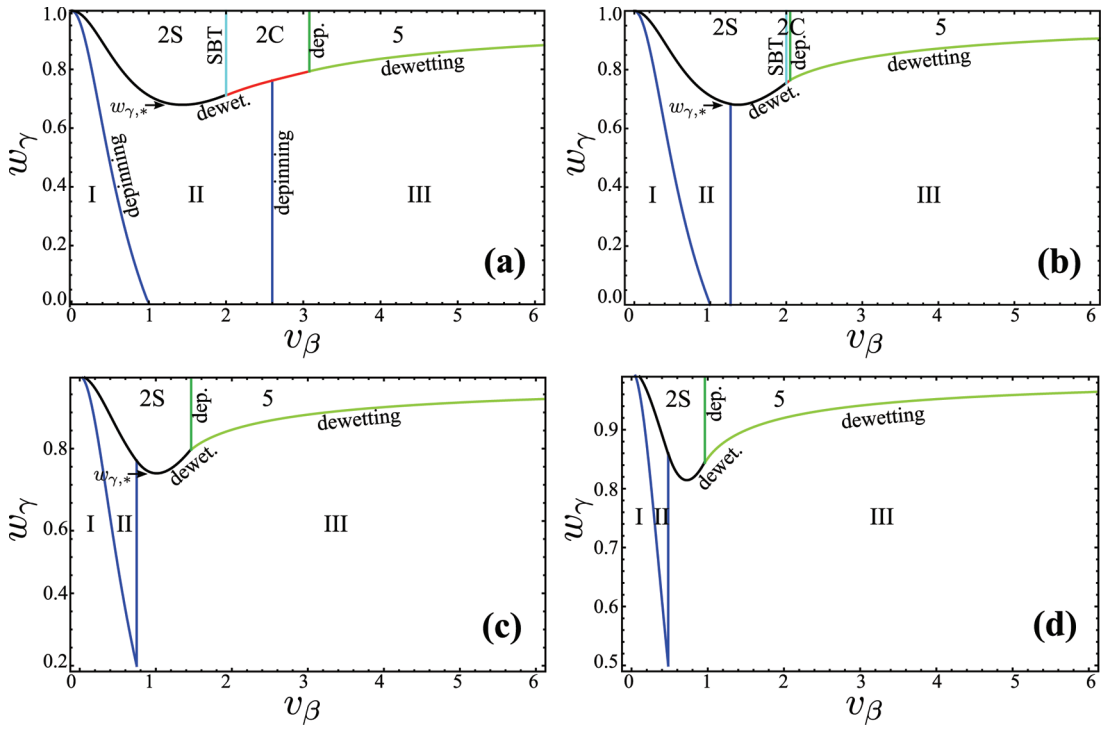

Figure 4. Morphology diagrams in the (v_β, w_γ) plane for four representative values of w_δ: (a) $w_\delta = -0.5 < w_{\delta,c-}$, (b) $w_\delta = -0.15$ with $w_{\delta,c} < w_\delta < w_{\delta,c}$, (c) $w_\delta = 0.2$ with $w_{\delta,c} < w_\delta < w_{\delta,c+}$, and (d) $w_\delta = 0.5 > w_{\delta,c+}$. In all four cases, $w_\gamma > 0$ and $w_\gamma > w_\beta$ as in eq 15. The morphology diagrams exhibit the three single-droplet morphologies I, II, and III as well as the three two-droplet morphologies 2S, 2C, and 5 as described in Figure 2. There are three types of morphological transitions: (i) continuous pinning and depinning transitions between the single-droplet regimes, (ii) discontinuous dewetting transitions from the two-droplet to the single-droplet regimes, and (iii) symmetry-breaking and depinning transitions between the two-droplet regimes. The continuous pinning and depinning transition lines between single-droplet regimes I, II, and III are shown as blue lines. The continuous symmetry-breaking transition (SBT) line between regimes 2S and 2C is shown as a vertical turquoise line and is present for $w_\delta < w_{\delta,c}$ in plots a and b. The depinning transition line between two-droplet regime 2S or 2C and two-droplet regime 5 is shown as a dark-green line. Dewetting transition lines are explained in the text.

Therefore, we use a different method and study corresponding bifurcations of the total volume v_β of both droplets as a function of the parameter $\cos\theta^{(1)}$ instead. This method is explained in more detail in the Supporting Information and is applied to obtain all instability lines and transition lines between two-droplet regimes. In the following text, we will present the main results of this analysis. Because for $w_\gamma = 1$ additional dewetting transitions into single-droplet morphologies are suppressed, the findings of this section are best summarized in a morphology and stability diagram in the (v_β, w_δ) plane for $w_\gamma = 1$ in Figure 3.

4.2.1. Symmetry-Breaking Transition 2S−2C. If the system starts in regime 2S with two equal droplets and we increase the volume, then a continuous symmetry-breaking transition (SBT) to morphology 2C takes place at the volume value of

$$v_{\beta,\mathrm{SBT}} = 2 \tag{16}$$

It is independent of wettabilities and thus is represented by a vertical turquoise line in all morphology and stability diagrams; see Figures 3−5 . This transition is the only morphological transition that is left if both domains are extremely lyophilic with $w_\gamma = 1$ and the substrate is extremely lyophobic with $w_\delta = -1$.[8] The existence of the SBT can be explained by the stability condition that at least one of the droplets must be pinned with a contact angle of $\theta < {}^{\pi}/_{2}$: for $v_\beta > 2$ and in symmetric configuration 2S, both droplets would become larger than half spheres with contact angles of $\theta > {}^{\pi}/_{2}$, which makes this state unstable.

4.2.2. Depinning Transitions 2S/2C−5. For increasing volume starting from regime 2S or 2C, the larger droplet can depin from the domain boundary and wet the δ substrate. This depinning transition depends only on the wettability w_δ of the surrounding substrate and the total volume v_β. Whereas depinning transitions between single-droplet morphologies I, II, and III are always continuous, depinning transitions between two-droplet morphologies can become *discontinuous*. Because the second pinned droplet, which must have a contact angle of $\theta^{(1)} < {}^{\pi}/_{2}$ to stabilize the configuration according to our above stability criterion (eq 14), has to remain in equilibrium with the depinning droplet it has to undergo the corresponding changes in Laplace pressure and thus radius of curvature. The depinning transition can become first order or can be replaced by a direct instability with respect to a single-droplet morphology if this results in a sufficiently large volume change of the pinned droplet in the opposite direction as the depinning droplet.

The analysis in the Supporting Information shows that the depinning transition can become discontinuous in a range of wettabilities $w_{\delta,c-} < w_\delta < w_{\delta,c+}$, where $w_{\delta,c-}$ and $w_{\delta,c+}$ determine two tricritical points of the morphology diagram. These tricritical points are at universal values of the wettability w_δ, which are obtained as solutions of the quartic equation

$$0 = 1 + {w_{\delta,c\pm}}^2 \mp w_{\delta,c\pm}(4 - 3w_{\delta,c\pm} + {w_{\delta,c\pm}}^3) \tag{17}$$

which leads to

$$w_{\delta,c-} \simeq -0.225, \quad w_{\delta,c+} = -1 + \sqrt{2} \simeq 0.414 \tag{18}$$

These values are universal because the depinning transitions are independent of the domain wettability w_γ and depend only on the wettability w_δ of the surrounding substrate.

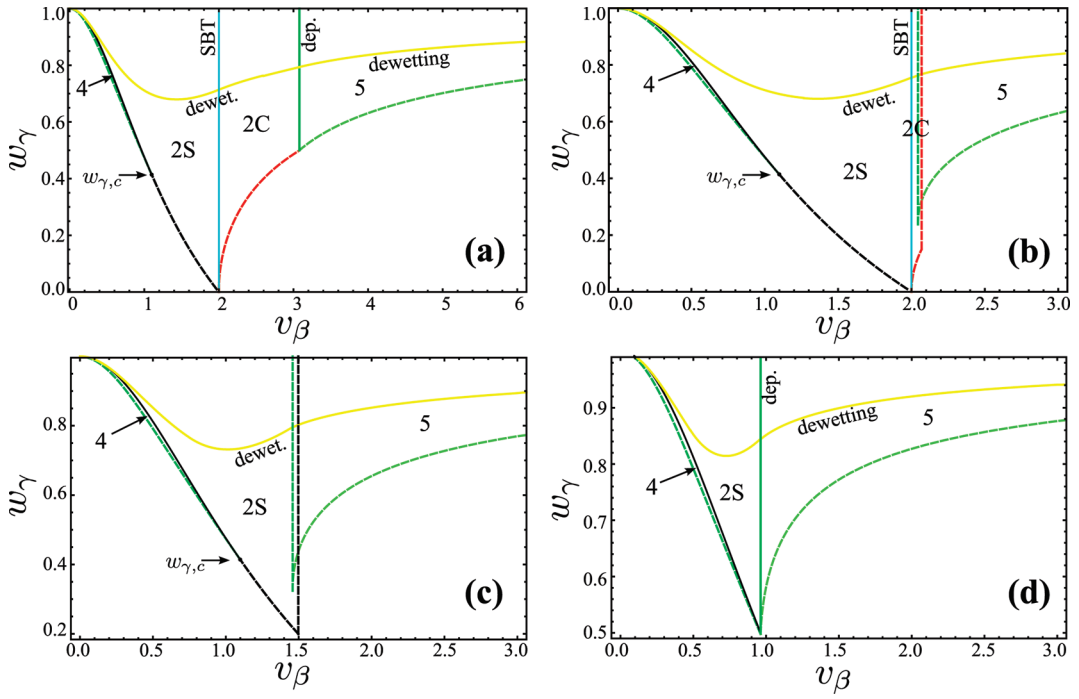

Figure 5. Stability diagrams of all metastable two-droplet regimes in the (v_β, w_γ) plane for four representative values of w_δ: (a) $w_\delta = -0.5 < w_{\delta,c-}$, (b) $w_\delta = -0.15$ with $w_{\delta,c-} < w_\delta < w_{\delta,c}$, (c) $w_\delta = 0.2$ with $w_{\delta,c} < w_\delta < w_{\delta,c+}$, and (d) $w_\delta = 0.5 > w_{\delta,c+}$. In all four cases, $w_\gamma > 0$ and $w_\gamma > w_\delta$ as in eq 15. The diagram shows the regions in the (v_β,w_γ) plane where two-droplet morphologies 2S, 2C, and 5 remain metastable. The solid yellow line represents the discontinuous transitions between single- and two-droplet regimes shown in the corresponding morphology diagrams in Figure 4 in black, red, and green. Instability lines are shown as dashed lines. The instability line of regime 4 with respect to dewetting is shown as a dashed dark-green line, and the instability lines of regime 2S with respect to dewetting (left) or depinning (right) are shown as dashed black lines. The vertical solid dark-green line between regimes 2S and 4 indicates the continuous depinning and symmetry-breaking transition between two metastable states 2S and 4 and ends at the critical point $w_{\gamma,c} = -1 + 2^{1/2}$ (arrows). The instability lines of regimes 2C and 5 with respect to dewetting or depinning are shown as dashed red lines and dashed dark-green lines, respectively.

In the Supporting Information, we also derive explicit results for the depinning transition lines between regimes 2C and 5 and between regimes 2S and 5. In the stability diagram in Figure 3, these depinning transition lines are shown as solid dark-green lines where the depinning is discontinuous and as solid black lines where it is continuous.

The transition line $v_{\beta,SBT} = 2$ of the continuous SBT between regimes 2S and 2C terminates in a critical endpoint on the line of discontinuous transitions between regimes 2S or 2C and regime 5. The corresponding critical wettability is also given by a universal value

$$w_{\delta,c} = \frac{6-\sqrt{51}}{10} \simeq -0.114 \qquad (19)$$

as derived in the Supporting Information. (For $w_\delta > w_{\delta,c}$ the SBT line continues as a transition line between metastable states. It terminates at $w_\delta = 0$, where it meets the instability line of the 2S regime.) This critical endpoint governs the morphology and stability diagram in the (v_β, w_δ) plane; see Figure 3. For substrate wettabilities $w_\delta < w_{\delta,c}$ there exist two distinct transitions: the SBT between regimes 2S and 2C and the depinning transition between regime 2C and 5. For a sufficiently lyophilic substrate with $w_\delta > w_{\delta,c}$, however, symmetry breaking and depinning of two droplets always happen in a *single* transition from regime 2S to regime 5.

The two tricritical points at universal values $w_{\delta,c-}$ and $w_{\delta,c+}$ together with the critical endpoint at the universal value $w_{\delta,c}$ define four representative parameter regimes of the substrate wettability w_δ: (a) $w_\delta < w_{\delta,c-}$, (b) $w_{\delta,c} > w_\delta > w_{\delta,c-}$, (c) $w_{\delta,c+} > w_\delta > w_{\delta,c}$, and (d) $w_\delta < w_{\delta,c+}$. For each parameter regime, we show additional morphology and stability diagrams in the (v_β, w_γ) plane for a fixed value of w_δ in Figure 4. For $w_\delta < w_{\delta,c-}$ in Figure 4a, there is a continuous depinning transition 2C−5; for $w_{\delta,c-} < w_\delta < w_{\delta,c}$ in Figure 4b, there is a discontinuous depinning transition 2C−5; for $w_{\delta,c} < w_\delta < w_{\delta,c+}$ in Figure 4c there is a discontinuous depinning transition 2S−5; and for $w_\delta > w_{\delta,c+}$ in Figure 4d, there is a continuous depinning transition 2S−5. In Figure 4c,d for $w_\delta > w_{\delta,c}$, depinning and symmetry breaking happen in a single transition.

4.2.3. Metastable Depinning Transition 2S−4. By starting from regime 2S and decreasing the volume, one of the droplets can depin from the domain boundary and retract to the γ domain. The detailed analysis given in the Supporting Information shows that regime 4 is only *metastable* and the transition between morphologies 2S and 4 is a depinning transition between metastable morphologies. Therefore, the corresponding depinning transition line and regime 4 itself do not appear in the morphology diagrams in Figure 3 or 4 but only in the stability diagrams in Figure 5, which are discussed in more detail below.

4.2.4. Bifurcation Diagram. For the experimental verifications of our results regarding the symmetry-breaking and depinning transition between two-droplet morphologies, a bifurcation diagram for two-droplet morphologies 2S, 2C, 4, and 5 is useful, where we plot the volume difference $\Delta v_\beta \equiv v_\beta^{(1)} - v_\beta^{(2)}$ as a function of the total volume v_β for each of the four two-droplet morphologies. This bifurcation diagram can be constructed in a parametric fashion using the results for volumes as a function of the parameter $\cos\theta^{(1)}$ given in the Supporting Information. The resulting bifurcation diagram Figure 6 shows *four* types of branches corresponding to the four two-droplet regimes 2S, 2C, 4, and 5 instead of only two branches, 2S and 2C, as for the case of extreme wettabilities $w_\gamma = 1$ and $w_\delta = -1$. Morphological

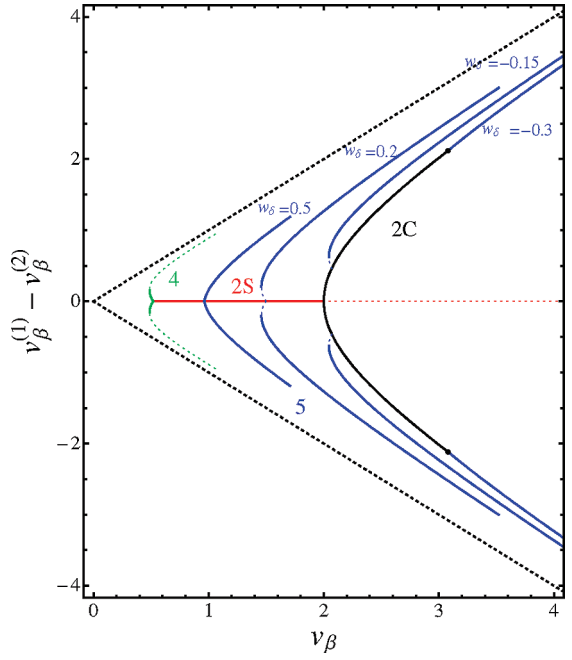

Figure 6. Bifurcation diagram showing the volume difference $\Delta v_\beta = v_\beta^{(1)} - v_\beta^{(2)}$ as a function of the total volume v_β for two-droplet regimes 2S (red line), 2C (black line), 4 (green line), and 5 (blue lines). For regime 4, we used $w_\gamma = 0.8$, and the four blue lines for regime 5 are generated for the four representative values $w_\delta = 0.5$, 0.2, −0.15, −0.3 (from left to right). Unstable branches are indicated by dotted lines. A morphological transition takes place where two lines meet. Single-droplet morphologies lie on the black dotted lines corresponding to $v_\beta^{(1)} = 0$ and $v_\beta^{(2)} = 0$.

transitions take place where two types of branches meet. The resulting branches can represent stable or metastable free-energy minima or unstable free-energy maxima. Unstable branches are indicated by dotted lines. Branch 2C ends where it meets the branch corresponding to regime 5. Endpoints of the lines that correspond to regime 4 or 5 represent the transitions into unstable morphologies 1, 3, or 6, which are not shown. The unstable branch corresponding to regime 4U represents the transition state for the transition from morphology 2S to single-droplet morphology.

4.3. Dewetting Transitions between Single- and Two-Droplet Morphologies. Finally, there are dewetting transitions, where one of the domains completely dewets resulting in a transition from a two-droplet into a single-droplet morphology. These transitions are studied by comparing the free energies of the corresponding two-droplet and single-droplet morphologies. Because these transitions represent transitions from a two-droplet minimum with $v_\beta^{(i)} > 0$ into a boundary minimum at $v_\beta^{(2)} = 0$ corresponding to a single-droplet regime, dewetting transition are always *discontinuous* and morphological hysteresis effects have to be studied. Therefore, we summarize our results both in morphology diagrams and corresponding stability diagrams in Figures 4 and 5 in the (v_β, w_γ) plane for four different values of w_δ. The four values for w_δ are chosen as representative of the four regimes arising from the above analysis of symmetry-breaking and depinning transitions between two-droplet morphologies: (a) $w_\delta < w_{\delta,c-}$, (b) $w_{\delta,c} > w_\delta > w_{\delta,c-}$, (c) $w_{\delta,c+} > w_\delta > w_{\delta,c}$, and (d) $w_\delta < w_{\delta,c+}$.

A dewetting transition into the single-droplet regime I is not possible. The volume of the corresponding initial two-droplet state would not be sufficient to support a stable two-droplet configuration with at least one pinned droplet. Therefore, only transitions between single-droplet morphologies II and III and

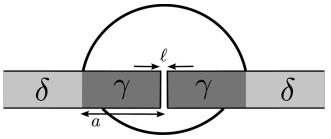

Figure 7. Plate with substrate wettability w_δ and circular lyophilic domains of radius a and wettability w_γ on both sides of the plate, which are connected by a cylindrical pore or capillary of small radius $l \ll a$.

two-droplet morphologies 2S and 2C are possible. Likewise, the total volume in two-droplet state 5 always exceeds the single-droplet depinning volume $v_{\beta,\mathrm{dep}}$; therefore, morphology 5 can dewet only into single-droplet morphology III. In the Supporting Information, we derive explicit expressions for the dewetting transition lines. Here we want to discuss the main features of these transition lines.

Transition lines $w_{\gamma,\mathrm{II-2S}}$ and $w_{\gamma,\mathrm{II-2C}}$ to single-droplet regime II and $w_{\beta,\mathrm{III-2S}}$, $w_{\beta,\mathrm{III-2C}}$, and $w_{\gamma,\mathrm{III-5}}$ to regime III join smoothly to give a single line of *discontinuous* transitions between the single- and two-droplet regimes, as can be seen in the morphology diagrams in Figure 4. This line is roughly horizontal because the dewetting transitions are driven by the competition between the interfacial energy and the contact energy if one of the domains dewets. This competition is governed by the wettability w_γ and depends only weakly on the volume v_β.

The dewetting transition lines $w_{\gamma,\mathrm{II-2S}}(v_\beta)$ and $w_{\gamma,\mathrm{III-2S}}(v_\beta)$ of regime 2S exhibit a minimum. For dewetting transition II−2S, this minimum is attained at a universal value

$$w_\gamma^* \simeq 0.678 \quad \text{and} \quad \theta_\gamma^* \simeq 47.3^\circ$$

$$v_\beta^* \simeq 1.443 \tag{20}$$

Along the first-order transition line, a Clausius−Clapeyron-like equation holds, which relates the slope of the transition line to the difference in Laplace pressure. At the minimum of the transition line, the Clausius−Clapeyron-like relation leads to the condition that morphologies on both sides of the transition line must have equal Laplace pressures. This means that at the minimum, the contact angles of morphologies 2S and II are complementary, $\cos\theta_{\mathrm{II}} = -\cos\theta_{2S}$. This additional condition leads to the above results (eq 20) as derived in the Supporting Information. It follows that below the critical wettability w_γ^* or for domain contact angles $\theta_\gamma > \theta_\gamma^*$ one of the domains *always* dewets, independently of the total volume.

The critical wettability w_γ^* in eq 20 is universal (i.e., independent of domain or substrate wettability) as long as the minimum in the transition line is attained for a dewetting transition from regime 2S to regime II. This phenomenon is reminiscent of the wetting morphologies for a striped surface domain, where for domain contact angles above a critical value of 38.2° the stripe partially dewets and the liquid always attains a bulged configuration instead of an extended channel configuration.[12] For a sufficiently lyophilic substrate δ with $v_{\beta,\mathrm{dep}} < v_\beta^*$ or $w_\delta > -0.226$, the minimum in the dewetting transition line of regime 2S is attained in regime III. Then, the resulting critical wettability w_γ^* is no longer universal but becomes an increasing function of the substrate wettability w_δ as derived in the Supporting Information.

The existence of a minimum in the transition line also leads to a *reentrance* of two-droplet regimes as a function of the total volume. These two phenomena are relevant for possible

applications involving controlled switching between single- and two-droplet morphologies.

These features of the dewetting transitions can be recognized in the morphology diagrams in Figure 4, which display the transition lines from regime 2S to regime II as a black line, from regime 2C to regime II or to regime III as a red line, and from regime 5 to regime III as a green line. The dewetting transition line has a minimum at wettability w_γ^* (indicated by arrows). For $w_\delta < -0.226$ in Figure 4a, this minimum is attained in regime II with the universal value $w_\gamma^* \simeq 0.678$; see eq 20. For $w_\delta > -0.226$ in Figure 4b−d, this minimum is attained in regime III and depends on the substrate wettability w_δ.

4.3.1. Instability Lines. We have shown that the dewetting transitions between two-droplet morphology 2S or 2C and single-droplet morphology II or III are always discontinuous, as well as some of the depinning transitions between two-droplet morphologies. Therefore, these transitions involve strong morphological hysteresis, which can be characterized by instability (or spinodal) lines of the different single- and two-droplet regimes, as shown in the stability diagrams in Figure 5 in the (ν_β, w_γ) plane for four different values of w_δ.

Single-droplet regimes I, II, and III correspond to boundary minima $\nu_\beta^{(2)} = 0$, which remain metastable for all domain wettabilities.

Regarding the dewetting transitions of the two-droplet morphologies, the instability mechanism for regime 2S for decreasing volume V_β exhibits an interesting behavior. Morphology 2S becomes unstable with respect to dewetting if $\cos\theta^{(i)} = w_\gamma$, and the droplets start to retract onto the γ domain. For high domain wettabilities w_γ, this retraction first leads to a depinning transition to morphology 4 (solid black line in Figure 5), which is only metastable as discussed above, before morphology 4 becomes unstable at a slightly smaller volume with respect to a dewetting transition into regime II or III (dashed dark-green line in Figure 5). The depinning transition into regime 4 is always continuous and depends only on the wettability w_γ of the lyophilic domain and the total volume ν_β. The analysis in the Supporting Information shows that a depinning transition from morphology 2S to morphology 4 is possible only for sufficiently lyophilic domains with $w_\gamma > w_{\gamma,c}$, where

$$w_{\gamma,c} = -1 + \sqrt{2} \tag{21}$$

is a critical point that is universal (i.e., independent of domain or substrate wettability). For low domain wettabilities $w_\gamma < w_{\gamma,c}$, there is a direct dewetting instability of the 2S state with respect to single-droplet morphology II or III (dashed black line in Figure 5) if the droplets start to retract onto the γ domain.

Upon increasing the volume ν_β, regime 2S becomes unstable with respect to depinning or symmetry breaking. According to the morphology and stability diagram in Figure 3, we have to distinguish three cases for the corresponding limits of stability of regime 2S. For $w_\delta > 0$, morphology 2S becomes unstable with respect to depinning if $\cos\theta^{(i)} = w_\delta$, i.e., if one of the droplets wets the δ substrate. For $w_\delta > w_{\delta,c}$ (Figure 5d), this instability coincides with the continuous depinning transition into regime 5 (solid dark-green line. For $0 < w_\delta < w_{\delta,c+}$ (Figure 5c), the resulting instability line (vertical dashed black line) is different from the discontinuous depinning transition line to regime 5. For $w_\delta < 0$ (Figure 5a,b), the continuous SBT transition line $\nu_{\beta,SBT} = 2$ gives the limit of stability of regime 2S for increasing volume ν_β.

Morphology 2C becomes unstable with respect to dewetting upon increasing the volume ν_β if the smaller droplet starts to retract onto the γ domain, $\cos\theta^{(1)} = w_\gamma$, resulting in a dewetting transition into single-droplet regime II or III (curved dashed red line in Figure 5a,b).

Morphology 2C becomes unstable with respect to depinning upon increasing the volume ν_β if the larger droplet starts wet the δ substrate, $\cos\theta^{(2)} = w_\delta$, resulting in a transition into regime 5. According to the morphology and stability diagram in Figure 3, we then have to distinguish two cases. For $w_\delta < w_{\delta,c-}$ (Figure 5a), this instability coincides with the continuous depinning transitions into regime 5 (solid dark-green line). For $0 > w_\delta > w_{\delta,c-}$ (Figure 5b), the resulting instability line (vertical dashed red line) is different from the discontinuous depinning transition line to regime 5.

Finally, morphology 5 can become unstable with respect to dewetting if the volume ν_β is increased such that the smaller droplet starts to retract onto the γ domain, $\cos\theta^{(1)} = w_\gamma$. This leads to dewetting into single-droplet regime III (dashed light-green lines in Figure 5).

Upon decreasing the volume ν_β, morphology 5 becomes unstable with respect to pinning if the larger droplet repins to the domain boundary for $\cos\theta^{(2)} = w_\delta$. According to the morphology and stability diagram Figure 3, we have to distinguish three cases. For $w_\delta < w_{\delta,c-}$ (Figure 5a), the instability coincides with the continuous pinning transition into regime 2C (solid dark-green line) and for $w_\delta > w_{\delta,c+}$ (Figure 5d), it coincides with the continuous pinning transition into regime 2C (solid dark-green line). For $w_{\delta,c-} < w_\delta < w_{\delta,c+}$ (Figure 5b,c), the resulting instability lines (vertical dashed dark-green lines) are different from the discontinuous depinning transition lines into regime 2S or 2C.

5. Summary and Discussion

5.1. Summary. We have derived all seven possible stable or metastable droplet morphologies by employing the stability criterion (eq 14) based on the volume dependence of the Laplace pressure, according to which states with two droplets can be stable only if at least one of the droplets is pinned and has a contact angle of $\theta < \pi/2$. Furthermore, we have achieved a complete classification of stable and metastable regimes by deriving morphology and stability diagrams both in the control parameter plane spanned by the total volume ν_β and the substrate wettability w_δ (Figure 3) and the plane spanned by the total volume ν_β and the domain wettability w_γ (Figures 4 and 5). The morphology diagrams are governed by three types of morphological transition lines: (i) depinning transitions of the contact lines, (ii) symmetry-breaking transitions, where the two droplets acquire different volumes, and (iii) dewetting transitions, where one domain dewets and one of the droplets vanishes.

Depinning and symmetry-breaking transitions give roughly vertical lines in the morphology diagrams in Figure 4 because they are mainly driven by volume change beyond a critical volume set by the geometry of the surface domain and are (roughly) independent of wettability. Dewetting transitions, however, give roughly horizontal lines in the morphology diagrams because they are driven by the competition between the interfacial energy and the contact energy if one of the domains dewets.

We find a qualitative difference between depinning transitions between single-droplet morphologies and depinning transitions between two-droplet morphologies: Whereas depinning transitions between single-droplet morphologies are always continuous, depinning transitions between two-droplet morphologies can become discontinuous. This qualitative change in depinning behavior is governed by two tricritical points in the

morphology diagram in Figure 3 at the universal substrate wettabilities $w_\delta = w_{\delta,c\pm}$; see eq 18. For $w_{\delta,c-} < w_\delta < w_{\delta,c+}$, the depinning transitions between morphologies 2S and 5 or morphologies 2C and 5 become discontinuous.

The symmetry-breaking transition between morphologies 2S and 2C is always continuous.[8] Depending on the substrate wettability w_δ, symmetry breaking and depinning can happen in a single transition between morphologies 2S and 5. This is the case above a critical substrate wettability $w_{\delta,c}$, which represents a critical endpoint of the symmetry-breaking transition lines between regimes 2S and 2C in the morphology diagram in Figure 3.

We also find that dewetting transitions between two- and single-droplet morphologies are always discontinuous and exhibit strong hysteretic effects that we quantified in the morphology and stability diagrams in Figures 4 and 5. The morphology diagrams also show that these dewetting transitions exhibit a reentrance because of a minimum in the corresponding transition line. Below the corresponding critical domain wettability w_γ^* in this minimum, one domain always dewets in equilibrium, independent of the total volume.

5.2. Experimental Realizations and Applications. Our findings should be accessible to experiments. Only recently, so-called capillary switches have been experimentally realized,[19−21] which consist of two droplets at the circular orifices of a small capillary with a diameter in the millimeter range.[20,21] In these realizations, volume exchange is achieved via the connecting capillary, which is much faster than volume exchange via a common vapor phase. Because these realizations are equivalent to two droplets on two circular domains with extreme wettabilities $w_\gamma = 1$ and $w_\delta = -1$, they exhibit only the symmetry-breaking transition between morphologies 2S and 2C at $\nu_{\beta,SBT} = 2$. Switching between the two morphologies 2S and 2C has been achieved in these systems either by additional pressure pulses applied to one of the droplets[20,21] or by electroosmosis.[19] Both techniques generated a pressure difference Δp between both droplets that gives an additional term in the free energy (eq 1) coupling to the volume difference $\Delta\nu_\beta = \nu_\beta^{(1)} - \nu_\beta^{(2)}$. This system has been used to verify a bifurcation diagram as shown in Figure 6 experimentally by measuring droplet volumes for different metastable configurations. For two droplets at circular orifices, as for the case of extreme wettabilities $w_\gamma = 1$ and $w_\delta = -1$, only the 2S and 2C regimes occur.

Our results for arbitrary wettabilities should be experimentally accessible using an analogous device consisting of a plate with substrate wettability w_δ and circular lyophilic domains of radius a and wettability w_γ on *both* sides of the plate. The domains are connected by a cylindrical pore or capillary of small radius $l \ll a$ in the middle of the domains (with the same wettability as the domains in the inner walls), which allows for fast volume exchange. For droplets much larger than the pore size l, imbibition of the liquid into the pore does not affect the overall shape of a single droplet on one side of the plate, and the pore is always filled because of constant Laplace pressure. Such a setup should allow us to verify the full bifurcation diagram in Figure 6 experimentally by measuring droplet volumes in different metastable configurations. In particular, such an experiment should find four branches corresponding to possible metastable two-droplet regimes 2S, 2C, 4, and 5 instead of only two branches 2S and 2C as for the case of extreme wettabilities $w_\gamma = 1$ and $w_\delta = -1$. The setup could also be combined with electrowetting techniques to allow control over wettabilities w_γ and w_δ,[13] and it should also be possible to determine morphology diagrams as shown in Figures 3 and 4 experimentally.

One particularly useful application of this setup is the controlled switching between single- and two-droplet morphologies. This could be achieved for wettabilities and volumes close to the corresponding discontinuous transition lines. Then additional pressure pulses Δp can induce switching between the coexisting metastable single- and two-droplet morphologies. The pressure difference Δp necessary to switch into two-droplet morphology is governed by the size of the pore. To create a second droplet of size l on the other side of the plate, which can depin from the pore boundary and wet the domain, a Laplace pressure on the order of $\Delta p \sim \Sigma_{\alpha\beta}/l$ is necessary. Finally, several plates can be placed in close proximity such that switching to a two-droplet morphology on both plates can induce the formation of a liquid bridge between both plates. By loading both plates with different reactants and inducing the formation of a liquid bridge, such a device could be used as a microreactor.

Acknowledgment. P.B. acknowledges support from the Marie Curie Early Stage Training Site, funded by the European Commission through the Marie Curie Human Resources and Mobility Activity Program, contract number MEST-CT-2004-504465.

List of Symbols

α	vapor phase
a	radius of the circular domain
$A_{\alpha\beta}$	area of the liquid−vapor interface
$\mathcal{A}_{\alpha\beta}$	surface of the liquid−vapor interface
$\mathcal{A}_{\beta\sigma}$	surface of the liquid−solid interface
β	liquid phase
δ	lyophobic substrate
ΔP	Laplace pressure
f	dimensionless free energy (eq 5)
γ	lyophilic substrate
l	pore size in Figure 7
M	mean curvature of the droplet
P_α	pressure of the vapor phase
P_β	pressure of the liquid phase
r	radius of the contact area of a spherical droplet
R	radius of curvature of a spherical droplet
σ	solid substrate
$\Sigma_{\alpha\beta}$	interfacial energy of the liquid−vapor interface
$\Sigma_{\alpha\sigma}$	interfacial energy of the vapor−substrate interface
$\Sigma_{\beta\sigma}$	interfacial energy of the liquid−substrate interface
θ	contact angle
$\theta^{(1)}$, $\theta^{(2)}$	contact angles of droplets 1 and 2
V_β	volume of the droplet
ν_β	dimensionless volume (eq 6)
$\nu_\beta^{(1)}$, $\nu_\beta^{(2)}$	dimensionless volumes of droplets 1 and 2
$w(\mathbf{x})$	local wettability (eq 4)
w_δ	w of the lyophobic matrix
w_γ	w of the lyophilic domain
$\mathbf{x}$	coordinate on the substrate

Supporting Information Available: Appendices with derivations of free energies for all droplet regimes, stability criterion for two-droplet morphologies, details on the bifurcation analysis method, and resulting expressions for transition lines and instability lines. This material is available free of charge via the Internet at http://pubs.acs.org.